Seeded Growth of Submicron Au Colloids with Quadrupole Plasmon Resonance Modes

Jessica Rodríguez-Fernández,[†] Jorge Pérez-Juste,*[,†] F. Javier García de Abajo,[‡] and Luis M. Liz-Marzán*[,†]

Departamento de Química Física, Universidade de Vigo, 36310 Vigo, Spain, and Centro Mixto CSIC-UPV/EHU and DIPC, Apartado 1072, 20080 San Sebastián, Spain

Received April 12, 2006. In Final Form: May 26, 2006

A modified seeded growth process has been used for the controlled synthesis of quasispherical, CTAB-stabilized gold nanoparticles from 12 up to 180 nm with narrow size distributions. The UV−visible spectra of the aqueous colloids show distinct bands corresponding to dipole and quadrupole plasmon modes, for diameters above 100 nm, in close agreement with predictions based on Mie theory. The assignment of the modes is demonstrated by calculation of near field enhancement maps based on the boundary element method. Apart from other applications, since absorption is drastically reduced above 600 nm, while scattering is largely increased, these particles open new possibilities for construction of highly efficient photonic structures.

Introduction

The optical properties of metal nanoparticles are dominated by collective oscillations of conduction electrons, termed surface plasmons. Whereas for small particles only dipolar modes are excited, with hardly any size dependence, as the particle size is increased above 50 nm, scattering (retardation) effects become more relevant, and the band is noticeably red-shifted and broadened.[1] When particle sizes above 100 nm are reached, dephasing starts to occur and new plasmon modes can be accommodated within the particle surface. These effects, which are important for a number of applications such as photonics,[2] photocatalysis,[3] or surface-enhanced Raman spectroscopy[4] have been recently demonstrated by Chumanov and co-workers for silver using a surfactant-less method involving reduction of silver oxide with a stream of H_2[5] and reaching particle sizes as large as 215 nm.[6] Higher order multipoles have also been reported for other geometries, such as Au shells,[7] Au and Ag rectangles,[8] and recently for triangular nanoprisms[9] and nanorods.[10] However, the sequential growth of spheroidal, reasonably monodisperse gold nanoparticles with sizes larger than 100 nm has been harder to achieve. Gold presents advantages mainly on the basis of a more robust chemical stability, which guarantees a long-term preservation of the optical features and allows for coating with thick silica shells without complications derived from ammonia-catalyzed oxidation.[11] A few papers have been published by Natan and co-workers on the seeded growth of Au nanoparticles, using mild reducing agents such as sodium citrate[12] or hydroxylamine,[13,14] obtaining particles between 20 and 100 nm in diameter, usually accompanied by a second population of nanorods amounting to ca. 5−10%. This work was followed up by Murphy's group,[15,16] using surfactant stabilizers and ascorbic acid as a reducing agent, which would subsequently become the basis for the first successful chemical synthesis of Au nanorods with reasonable yields,[17] but only allowed the growth of monodisperse spheres up to 40 nm. Large (micron sized) gold spheres have been reported by Goia and Matijevic but were always claimed to be composed of aggregated small nanoparticles.[18] In this paper, we report the seeded growth of gold spheres with narrow size distributions. Results are shown for diameters up to 181 nm, but there is no reason against carrying out subsequent growth steps and achieving larger particles.

Experimental Section

Chemicals. Ascorbic acid and cetyltrimethylammonium bromide (CTAB) were supplied by Aldrich. $HAuCl_4 \cdot 3H_2O$ and trisodium citrate dihydrate were supplied by Sigma. All reactants were used without further purification. Water was Milli-Q grade.

Particle Synthesis. Seeds (12 nm, 0.5 mM) were prepared by citrate reduction and then diluted with the same volume of a 0.03 M CTAB solution. The first growth step was carried out by addition of ascorbic acid solution (5×10^{-4} M) onto a mixture of $HAuCl_4$ (2.5×10^{-4} M) and CTAB (0.015 M) at 35 °C, followed by addition of the seed solution ([Au] = 2.31×10^{-6} M). Since in this first step of the growth, nanorods and planar shapes are obtained along with spheres, purification was carried out following the method reported by Jana.[19] However, in this work, it was the supernatant (basically free of nonspherical particles) which was subsequently used for further growth by means of the same procedure described for seed

* To whom correspondence should be addressed. Fax: +34 986812556. E-mail: juste@uvigo.es (J.P.-J.); lmarzan@uvigo.es (L.M.L.-M.).
† Universidade de Vigo.
‡ Centro Mixto CSIC-UPV/EHU and DIPC.

(1) Link, S.; El-Sayed, M. A. *J. Phys. Chem. B* **1999**, *103*, 8410.
(2) Moroz, A. *Phys. Rev. Lett.* **1999**, *83*, 5274.
(3) Kamat, P. V. *J. Phys. Chem. B* **2002**, *106*, 7729.
(4) Xu, H.; Bjerneld, E. J.; Käll, M.; Börjesson, L. *Phys. Rev. Lett.* **1999**, *83*, 4357.
(5) Evanoff, D. D., Jr.; Chumanov, G. *J. Phys. Chem. B* **2004**, *108*, 13948.
(6) Kumbhar, A. S.; Kinnan, M. K.; Chumanov, G. *J. Am. Chem. Soc.* **2005**, *127*, 12444.
(7) Oldenburg, S. J.; Hale, G. D.; Jackson, J. B.; Halas, N. J. *Appl. Phys. Lett.* **1999**, *75*, 2897.
(8) Krenn, J. R.; Schider, G.; Rechberger, W.; Lamprecht, B.; Leitner, A.: Aussenegg, F. R.; Weeber, J. C. *Appl. Phys. Lett.* **2000**, *77*, 3379.
(9) Shuford, K. L.; Ratner, M. A.; Schatz, G. C. *J. Chem. Phys.* **2005**, *123*, 114713.
(10) Payne, E. K.; Shuford, K. L.; Park, S.; Schatz, G. C.; Mirkin, C. A. *J. Phys. Chem. B* **2006**, *110*, 2150.
(11) Ung, T.; Liz-Marzán, L. M.; Mulvaney, P. *Langmuir* **1998**, *14*, 3740.
(12) Brown, K. R.; Natan, M. J. *Langmuir* **1998**, *14*, 726.
(13) Brown, K. R.; Lyon, L. A.; Fox, A. P.; Reiss, B. D.; Natan, M. J. *Chem. Mater.* **2000**, *12*, 314.
(14) Brown, K. R.; Walter, D. G.; Natan, M. J. *Chem. Mater.* **2000**, *12*, 306.
(15) Jana, N. R.; Gearheart, L.; Murphy, C. J. *Langmuir* **2001**, *17*, 6782.
(16) Jana, N. R.; Gearheart, L.; Murphy, C. J. *Chem. Mater.* **2001**, *13*, 2313.
(17) Jana, N. R.; Gearheart, L.; Murphy, C. J. *J. Phys. Chem. B* **2001**, *105*, 4065.
(18) Goia, D. V.; Matijevic, E. *New J. Chem.* **1998**, *22*, 1203.
(19) Jana, N. R. *Chem. Commun.* **2003**, 1950.

10.1021/la060990n CCC: $33.50
Published on Web 06/29/2006

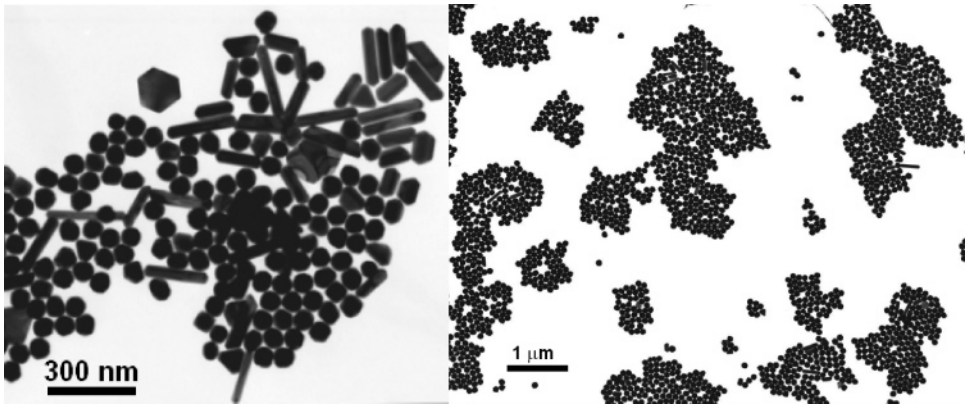

Figure 1. Representative TEM micrographs of Au nanoparticles grown from 12 nm seeds, before (left) and after (right) the purification step.

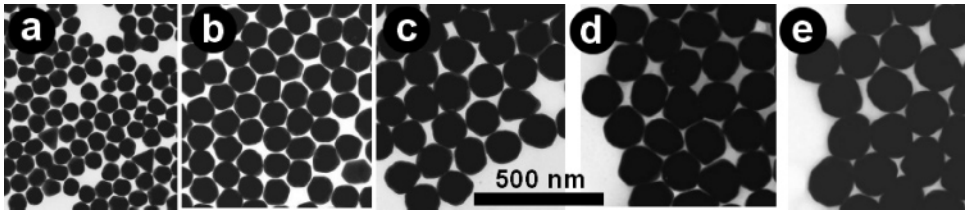

Figure 2. Representative TEM micrographs of Au spheres obtained after subsequent growth steps. Average diameters are 66 (a), 100 (b), 139 (c), 157 (d), and 181 (e) nm.

growth. The concentrations were adjusted to achieve predetermined final sizes.

Experimental Techniques. A JEOL JEM 1010 transmission electron microscope operating at an acceleration voltage of 100 kV was used for particle sizing. SEM characterization was carried out with a JEOL JSM-6700F FEG-SEM operating at an acceleration voltage of 5 kV for acquisition of secondary electrons images (SEI).

UV−vis spectra were measured with an Agilent 8453 UV−Vis diode-array spectrophotometer.

Optical Modeling. Simulations of absorption spectra were performed using Mie theory based upon spherical wave expansion of the fields inside and outside a spherical particle.[20] Near-field enhancement maps were obtained using the boundary element method (BEM)[21,22] and further confirmed with Mie theory calculations. In the BEM, the electromagnetic fields are expressed in terms of surface integrals involving charge and current distributions defined on the particle surface. The boundary conditions of the electromagnetic fields are then imposed to yield a set of self-consistent surface integral equations that determine the surface sources and that are solved by discretizing the surface through a finite number of representative boundary points. This leads to a linear set of equations that is solved by linear algebra techniques.

Results and Discussion

The synthetic procedure we are reporting here basically develops from the earlier work on CTAB assisted seeded growth and more specifically from our previous study on the synthesis and mechanism of gold nanorod formation,[23] but definitely overcoming the limitations originally believed to arise from capping molecules[6] and tuning the experimental conditions to favor the formation of spheres over other shapes such as rods and prisms.[12,15] Two key modifications have been included in the seeded growth of smaller gold nanoparticles by ascorbic acid reduction of $HAuCl_4$, namely the reduction was carried out at an increased temperature of 35 °C and a purification step was introduced after the first growth step to get rid of (most of) the nonspherical particles obtained as a byproduct. Although the higher temperature favors isotropic over one-dimensional growth and rod formation,[23] the early removal of particles with other morphologies is decisive to maintain a quasispherical geometry during subsequent growth steps. Other factors affecting the way in which growth occurs are the use of lower CTAB concentration and larger ascorbic acid concentration, as compared to those used for nanorod growth. In Figure 1, TEM micrographs are shown of the particles obtained after the first growth step, both before and after purification. Although a noticeable amount of nonspherical shapes form during the first seeded growth process (ca. 35% as estimated from TEM images), upon purification, they are observed to have been removed almost completely (<6% nonspherical particles estimated from TEM images). Figure 1b clearly reveals the uniform size of the gold spheres, which have a size of 66.5 ± 9.3 nm. The spectral changes derived from this purification process are shown in the Supporting Information (Figure S1).

Using the particles shown in Figure 1b as seeds, further growth steps were carried out, again by reduction of $HAuCl_4$ with ascorbic acid in the presence of CTAB at 35 °C. As a result, particles with average sizes of 100.7 ± 10.9, 139.2 ± 6.8, 157.6 ± 9.5, and 181.2 ± 11.7 nm were produced, and the uniformity of each sample is exemplified in the TEM micrographs shown in Figure 2. Although the particles are rather faceted, and thus not perfectly spherical, the growth is very uniform up to almost 200 nm, without formation of elongated particles. We have no reason to believe that this is the largest size available, since in principle additional growth steps can be carried out in the same manner.

An issue that needs to be addressed before discussing the optical properties of the obtained gold hydrosols is whether we are dealing with single particles or rather with aggregates of smaller units forming compact aggregates, as was found by Goia and Matijevic.[18] This was investigated using high magnification SEM. Examples of the images obtained for the largest size prepared are shown in Figure 3 at magnifications as high as 50 000× and 85 000×. The faceted structure is evident, as well as the smoothness of all surfaces, clearly indicating that we have

(20) Jackson, J. D. *Classical Electrodynamics*; Wiley: New York, 1975.
(21) García de Abajo, F. J.; Howie, A. *Phys. Rev. Lett.* **1998**, *80*, 5180.
(22) García de Abajo, F. J.; Howie, A. *Phys. Rev. B* **2002**, *65*, 115418.
(23) Pérez-Juste, J.; Liz-Marzán, L. M.; Chan, D. Y. C.; Carnie, S.; Mulvaney, P. *Adv. Funct. Mater.* **2004**, *14*, 572.

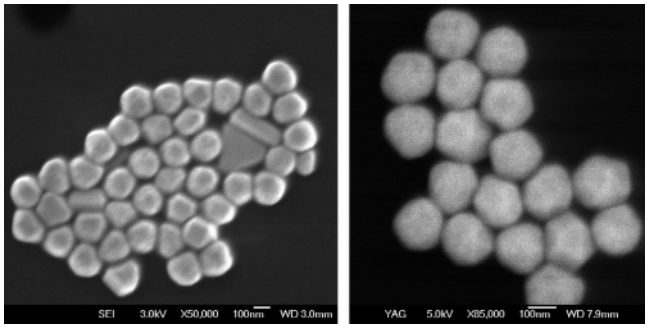

Figure 3. SEM micrographs of Au spheres (average diameter 181 nm) at two different magnifications. The smoothness of the surface reveals uniform growth on the initial seeds.

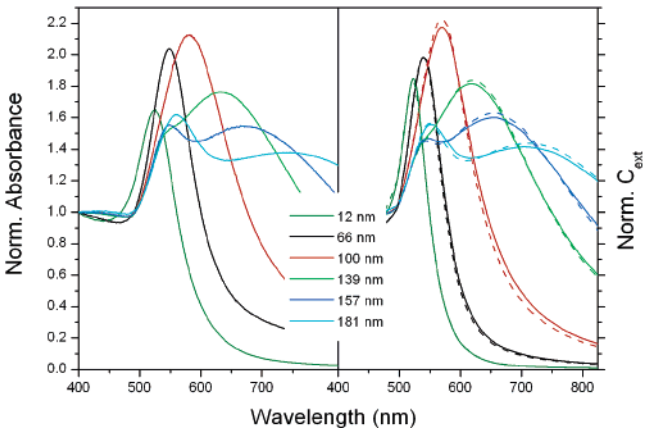

Figure 4. (a) UV−visible spectra of Au colloids with various average diameters. (b) Calculated (Mie theory) extinction spectra of dispersions containing Au spheres with the same size distributions as the experimental colloids (solid lines) and for monodisperse spheres with the average particle size (dashed lines). All spectra are normalized at 400 nm to facilitate comparison.

single particles with quasispherical, polyhedral morphology, as previously observed for large silver particles.[6] Although a few particles with rod or platelike geometry can be sometimes observed, the proportion is extremely low and thus are not expected to significantly contribute to the optical response of the dispersion.

The optical properties of the colloids containing the particles shown in Figure 2 were determined by UV−visible spectroscopy in absorbance mode. The measured spectra were plotted in Figure 4a upon normalization at 400 nm, where absorbance is mainly due to interband transitions, thus facilitating comparison. The spectrum for standard, CTAB-stabilized 12 nm nanoparticles is also included. The observed trend agrees very well with the expected changes in optical behavior for increasing particle sizes, as described in the Introduction. After an initial red-shift (from 525 up to 548 nm) between 12 and 66 nm particles, when the diameter is increased up to 100 nm, there is a noticeable red-shift up to 581 nm and band broadening, but still with a single band. Above 100 nm, a shoulder starts to develop at lower wavelengths, corresponding to a quadrupolar resonance as the main (dipolar resonance) band red-shifts and broadens further, peaking at 632 nm for an average diameter of 139 nm. Even broader dipolar bands centered at lower energies (670 and 747 nm) and well-defined quadrupolar resonances (peaking at 548 and 560 nm) are measured for larger particles of 157 and 181 nm average diameter, respectively.

These results can be directly compared with calculations based on the standard Mie theory for spherical particles.[24] For the calculation of the extinction spectra (containing both absorption and scattering contributions, so as to be compared with the experimental absorbance data) shown in Figure 4b, averaging over the contributions of various populations measured from TEM images of each experimental sample was carried out, thus providing a slightly better agreement than the comparison with spectra calculated for spheres with the experimental average particle size (spectra included in the figure as dashed lines). In both cases, the agreement is actually better than expected,[25] taking into account the small deviation from the spherical shape observed in the TEM images. The broadening of the dipole plasmon band stems mainly from radiative losses: the mode cannot be trapped in the particle and it couples to freely propagating light (this is ultimately the reason it couples to the incoming light), leading to a width that increases with the strength of the coupling, which is in turn increased with particle size.

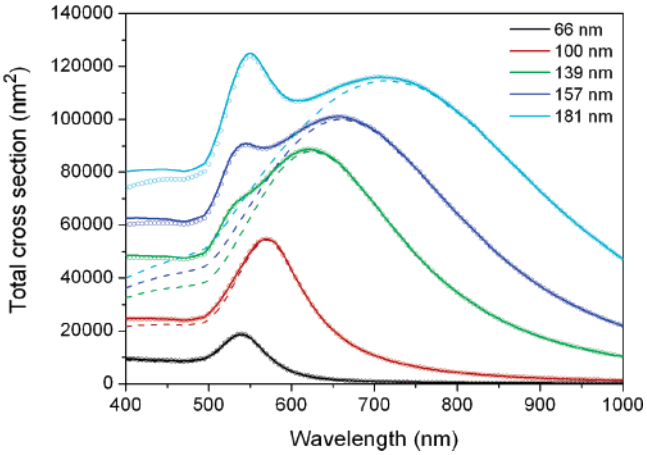

Figure 5. Total absorption cross section of Au spheres with various diameters (as labeled). Full lines were calculated with multipoles up to $l = 12$, whereas dashed lines correspond to $l = 1$ (only dipoles) and symbols to $l = 1,2$ (dipoles and quadrupoles).

The above assignment of the dipole and quadrupole modes is confirmed by calculations restricted to just dipolar or quadrupolar Mie modes, as shown in Figure 5, where the calculations restricted to dipoles (dashed curves) exhibit just the dipolar band and work extremely well for small particles, whereas inclusion of quadrupoles (symbols) results in both the additional quadrupolar feature (band/shoulder) that shows up as the particle size increases and nonnegligible corrections in the dipolar feature. The contribution of high-order multipoles can be disregarded for the particle sizes under consideration.

This picture is further illustrated by calculating the near field enhancement when the larger particles are illuminated with light of the respective maximum wavelengths. Such calculations were carried out using the boundary element method (BEM),[21,22] in which the induced electric and magnetic fields are viewed as originating from equivalent boundary sources (i.e., equivalent surface electric charges and currents), which are used to fulfill the customary boundary conditions at the interfaces between different media. The results obtained for spheres of 12, 66, and 180 nm diameter are shown in Figure 6, clearly demonstrating a dipolar mode for the single band of the smaller particles but dipolar and quadrupolar modes for the long and short wavelength bands, respectively, in the larger particle (see induced-charge patterns in Figure S2 of the Supporting Information).

(24) Bohren, C. F.; Huffman, D. R. *Absorption and Scattering of Light by Small Particles*; Wiley: New York, 1983.

(25) The positions of the maxima for the calculated dipole (quadrupole) modes are 523, 540, 570, 618, 655 (545), and 707 (551) for average diameters of 12, 66, 100, 139, 157, and 181 nm, respectively.

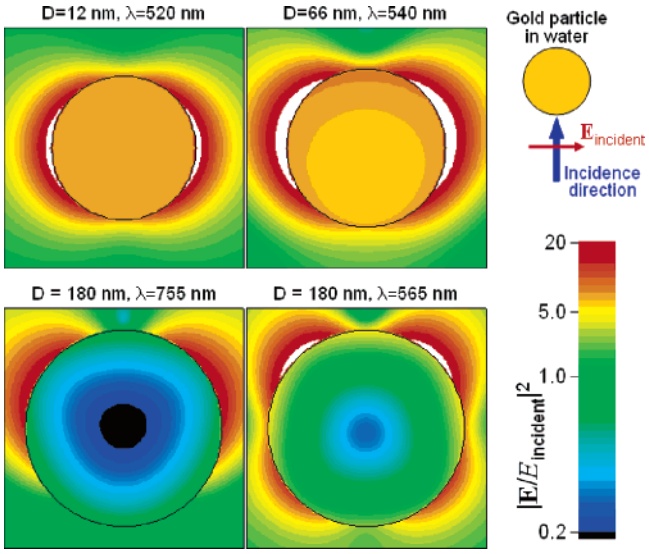

Figure 6. Near field enhancement at spherical gold nanoparticles of various size in water, when illuminated at their corresponding plasmon wavelengths. The polarization and illumination directions are schematically shown.

Further analysis of Mie theory shows that the asymmetry observed in both dipolar and quadrupolar modes of the larger spheres arise from mixing of the dipolar component along the incident field direction *x* and the quadrupolar component with *xz* symmetry. In both cases, mode mixing arises from retardation: the particle size is no longer much smaller than the wavelength, and as a result, the incident field is sufficiently inhomogeneous across the extension of the particle to allow coupling with the *xz* component. This is illustrated more explicitly in the Supporting Information (Figure S2). Retardation is less effective in quadrupolar components (see Figure 6), since they involve surface charge distributions with more sign changes. Actually, the dipolar mode shifts considerably further with particle size and undergoes more pronounced broadening. Similar effects and conclusions have been reported by Schatz and co-workers for silver spheres.[26]

It is important to bear in mind that, as particle size increases, the main contribution to extinction for wavelengths above ca. 600 nm comes from scattering, with nearly negligible absorption. Calculated spectra for the specific contributions of absorption and scattering to the optical response for spheres between 70 and 180 nm are provided as Supporting Information (Figure S3). From these plots, it is clear that the construction of photonic crystals containing such particles as building blocks can profit from excellent dielectric contrast with minimal absorption, as far as the photonic band gap is tuned at the higher wavelength side of the visible spectrum, or into the near-IR, which can be achieved through growth of silica shells with the appropriate thickness.[27,28]

Conclusions

Quasispherical gold colloids with low polydispersity can be synthesized using a fairly simple seeded growth process in aqueous solution, with a tight control on particle size and with optical properties that can be accurately predicted using the standard Mie theory for spheres. The assignment of the plasmon modes was confirmed using near field enhancement calculations based on the boundary element method. The huge scattering contribution for larger spheres makes them good candidates for photonic crystal applications, which will be reported elsewhere.

Acknowledgment. This work has been funded by the Spanish Ministerio de Educación y Ciencia through Project No. NAN2004-08843-C05-03/05 and through an F.P.U. scholarship (J.R.-F.). B. Rodríguez-González is thanked for acquiring the SEM images.

Supporting Information Available: UV−vis spectra of the sample obtained after the first growth step, before and after purification (Figure S1). Illustration of the coupling of *x*-polarized incident light to *x* and *xz* multipolar components in the spheres (Figure S2). Calculated spectra for the absorption and scattering coefficients of gold nanospheres of different diameters (Figure S3). This material is available free of charge via the Internet at http://pubs.acs.org.

LA060990N

(26) Kelly, K. L.; Coronado, E.; Zhao, L. L.; Schatz, G. C. *J. Phys. Chem. B* **2003**, *107*, 668.

(27) García-Santamaría, F.; Salgueiriño-Maceira, V.; López, C.; Liz-Marzán, L. M. *Langmuir* **2002**, *18*, 4519.

(28) Graf, C.; van Blaaderen, A. *Langmuir* **2002**, *18*, 524.

Seeded Growth of Submicron Au Colloids with Quadrupole Plasmon Resonance Modes

Jessica Rodríguez-Fernández[1], Jorge Pérez-Juste[1,*], F. Javier García de Abajo[2], and Luis M. Liz-Marzán[1,*]

[1]Departamento de Química Física, Universidade de Vigo, 36310 Vigo, Spain

Fax: +34 986812556. E-mail: juste@uvigo.es; lmarzan@uvigo.es

[2] Centro Mixto CSIC-UPV/EHU and DIPC, Apartado 1072, 20080 San Sebastián, Spain

SUPPORTING INFORMATION

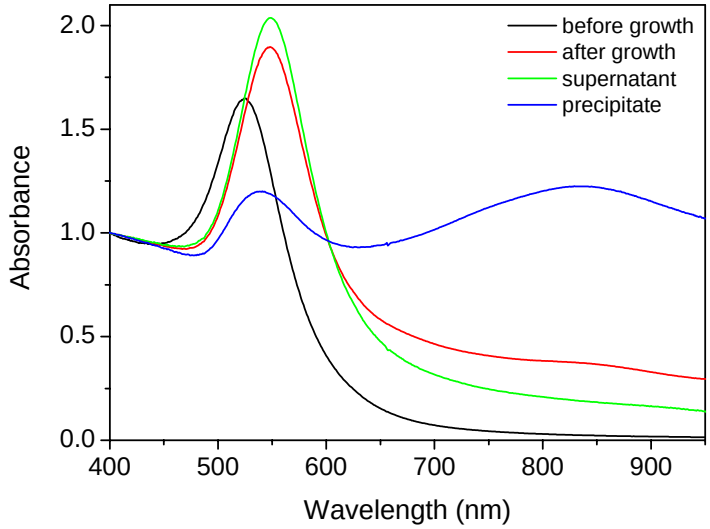

Figure S1. UV-vis spectra of the sample obtained after the first growth step, before (red) and after (green) purification. The blue spectrum was measured after redispersion of the precipitate. The spectrum of the seeds (black line) is shown as reference. All spectra were normalized at 400 nm.

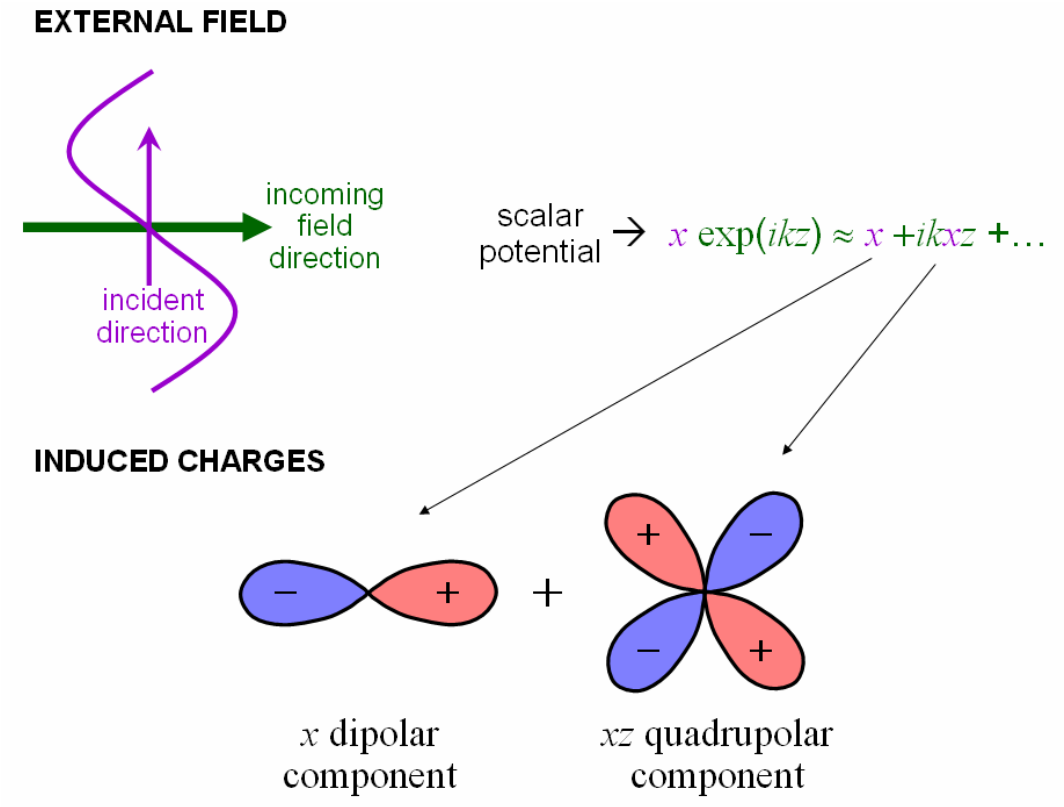

Figure S2. Illustration of the coupling of *x*-polarized incident light to *x* and *xz* multipolar components in the spheres. The scalar potential associated to the external field has both of these components, the *z* dependence arising from the wave modulation along the propagation direction, which becomes noticeable as the particle size increases. In terms of multipoles, the *x* component arises as a superposition of (l=1, m=±1), whereas the *xz* component is a combination of (l=2, m=±1), and other values of the azimuthal number *m* are forbidden by symmetry.

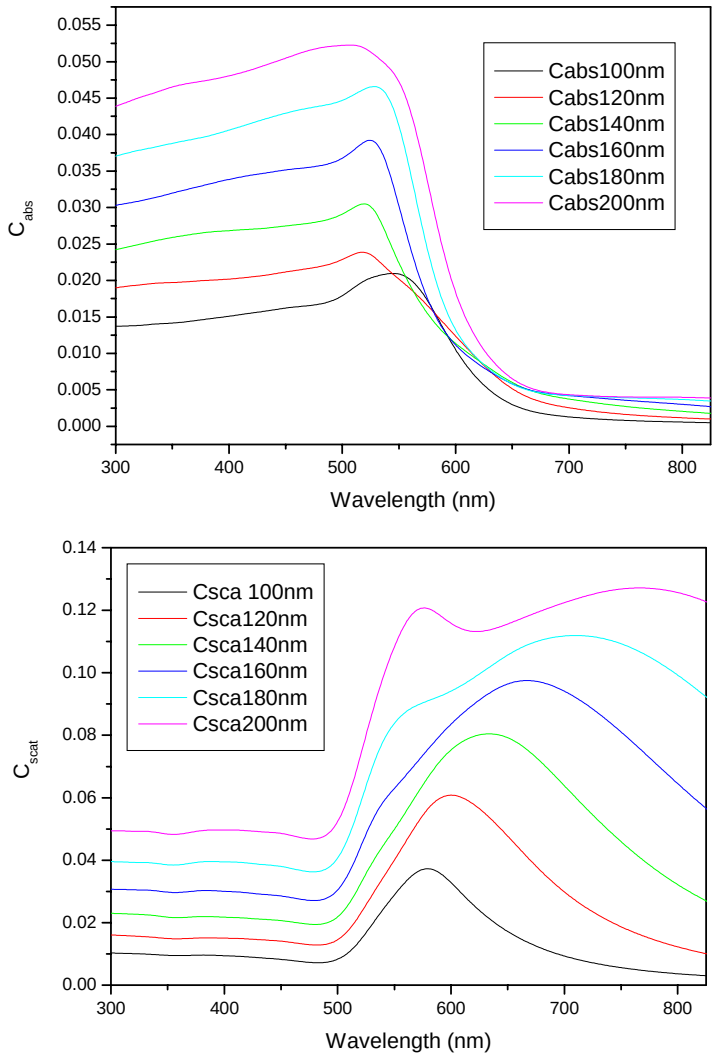

Figure S3. Calculated spectra for the absorption (top) and scattering (bottom) coefficients of gold nanospheres of different diameters, as indicated in the labels.